Mineral. Deposita 30, 439–448 (1995)

MINERALIUM DEPOSITA

Effects of greenschist-facies metamorphism and related deformation on the Mobrun massive sulfide deposit, Québec, Canada

A.C.L. Larocque*, C.J. Hodgson

Department of Geological Sciences, Queen's University, Kingston, Ontario K7L 3N6, Canada

Received: 8 June 1994/Accepted: 21 October 1994

Abstract. The Mobrun Zn-Cu-Ag-Au deposit in the Noranda mining camp is hosted by Archean mafic and felsic submarine volcanic rocks. The deposit comprises three massive sulfide complexes: the Main and Satellite Lenses near surface, and the 1100 orebody at depth. The rocks have been subjected to lower greenschist-facies metamorphism and related deformation, which resulted in changes in ore textures, development of shear zones and veins systems, remobilization of gold, and formation of a new mineral (electrum) within the orebodies. Both mechanical and chemical processes operated to produce secondary textures and structures resulting from brittle deformation, ductile deformation, and annealing. The specific deformation mechanisms include brittle failure and cataclastic flow, dislocation glide, dislocation creep and solution-precipitation creep. The Main and Satellite Lenses are characterized by excellent preservation of primary sulfides deposited from and reworked by synvolcanic hydrothermal fluids. These orebodies were affected to a limited degree by mechanical processes of deformation. In contrast, the 1100 orebody is characterized by a higher degree of development of textures and structures related to metamorphism and deformation, especially those formed by chemical processes. The differences may be due to the greater depth of the 1100 orebody relative to the other lenses, as regional metamorphic isograds are subhorizontal, and more extensive interaction between metamorphic fluids and the 1100 Lens.

Deformation experiments on natural polycrystalline sulfides have provided information on their mechanisms of deformation. Under greenschist-facies metamorphic conditions, pyrite deforms exclusively by cataclasis (Atkinson 1975; Cox et al. 1981). In contrast, chalcopyrite and sphalerite deform ductilely, by intragranular (dislocation) sliding and deformation twinning (Clark and Kelly 1973; Kelly and Clark 1975; Roscoe 1975). Pyrrhotite, which undergoes brittle deformation at low temperature and pressure, deforms ductilely by twin-gliding at temperatures above 250°C (Clark and Kelly 1973). Interpretation of deformation textures may be made difficult by the fact that evidence of ductile deformation in sulfides may be obliterated by subsequent static (postdeformational) recrystallization or thermal annealing. This is especially common in pyrrhotite.

Examining the effects of deformation on monomineralic sulfide aggregates is useful, as it provides information about the relative importance of diffusion, slip, and intergranular deformation (Poirier 1985). However, the behaviour of individual sulfide minerals during metamorphism and related deformation of massive sulfide deposits may vary greatly, depending on temperature, strain rate, confining pressure, fluid pressure, differential stress, permeability within the zone of deformation, and the nature of adjacent or matrix-forming sulfides (Ashby and Verrall 1973; Kelly and Clark 1975; Knipe 1989; Cook et al. 1993; Duckworth and Rickard 1993). Cox (1987) subdivided deformation mechanisms in sulfide minerals into the following categories: 1) brittle failure and cataclastic flow; 2) low-temperature plasticity (dislocation glide and mechanical twinning); 3) dislocation creep; 4) solution-precipitation creep; 5) solid-state diffusion creep; and 6) grain-boundary sliding. The effects of metamorphism and deformation on massive sulfide deposits have been described by many authors (Vokes 1969; Mookherjee 1976; McClay 1991; Craig and Vokes 1992, 1993; Vokes and Craig 1993, among others).

The general effects of metamorphism and deformation on rocks comprise chemical/mineralogical changes, textural changes, and structural changes. In their study of sulfide deposits in the Appalachian – Caledonian Orogen, Craig and Vokes (1992) observed that metamorphism ranging from greenschist- to amphibolite-facies had little effect in altering the mineralogy; however, metamorphism had a significant effect on ore textures and the distribution of minor elements among co-existing minerals. Similarly,

* *Present address*: Department of Geological Sciences, University of Manitoba, Winnipeg, Manitoba R3T 2N2, Canada

greenschist-grade metamorphism of the Mobrun volcanogenic massive sulfide (VMS) deposit resulted in changes in ore textures, development of tectonic structures, and remobilization of ore constituents. The purpose of this paper is to describe these changes, and to discuss the specific mechanisms responsible.

Regional geology

The Mobrun deposit is one of a group of VMS deposits within the Noranda mining camp hosted by interbedded mafic and felsic submarine volcanic rocks of the Archean Blake River Group (BRG) in the south-central part of the Abitibi Greenstone Belt (de Rosen-Spence 1976). The BRG is the uppermost volcanic sequence in the southern part of the belt and is underlain by tholeiitic flows of the Kinojevis Group in the eastern segment of the belt (Ministère de l'Energie et des Ressources du Québec – Ontario Geological Survey 1984). Both groups have been folded into the Blake River Synclinorium (BRS), a large-scale east-trending structure. The BRS is bounded by regional high-angle reverse faults, the Porcupine – Destor Break on the north and the Larder Lake – Cadillac Break on the south.

The area has been affected by two main periods of deformation, designated D1 and D2 (Dimroth et al. 1983a; Hubert et al. 1984). Most of the Noranda camp is located on the gently dipping upright limb of one of a number of large-scale northwest-trending F1 folds. No penetrative cleavage is associated with D1 folds; however, D1 faults typically are marked by bedding-parallel zones of schistosity possibly formed during D2. The main cleavage-forming event (D2) resulted in east-west-trending folds and an associated domainal cleavage. The most intense D2 deformation is localized along the Larder Lake – Cadillac Break, a structure which appears to post-date F1 folds but pre-date D2.

Metamorphic grades in the BRG generally range from prehnite-pumpellyite to greenschist facies (Jolly 1980; Dimroth et al. 1983b; Gélinas et al. 1984). Amphibolite facies assemblages which overprint greenschist assemblages occur in the contact metamorphic aureoles of syn- to late-tectonic intrusions (Gélinas et al. 1984). In the Noranda area, greenschist facies assemblages dominate. Locally, these overprint hornblende hornfels facies assemblages developed in aureoles of stocks (Jolly 1978; Riverin and Hodgson 1980).

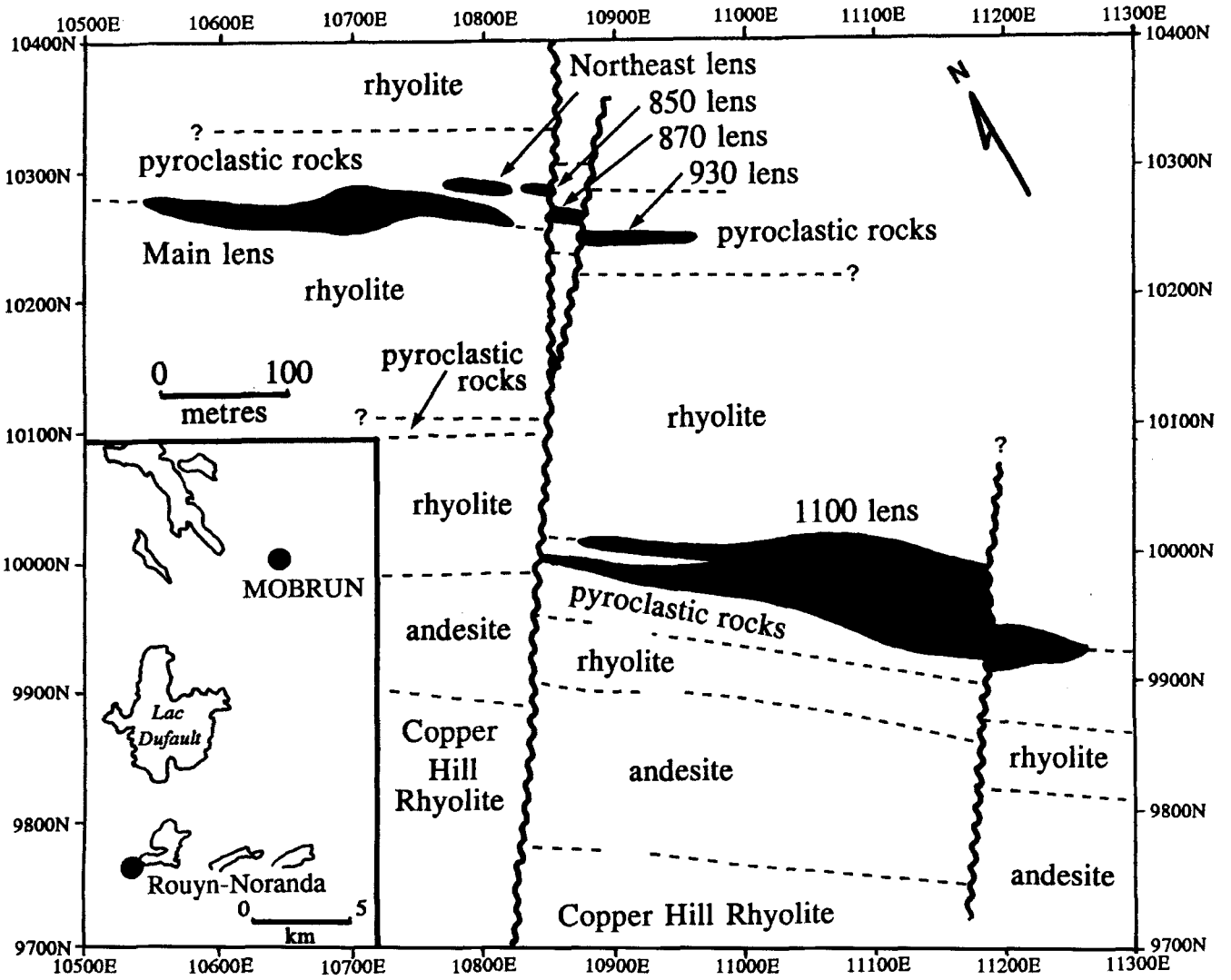

Fig. 1. Geology of the Mobrun deposit, modified from Caumartin and Caillé (1990). *Inset*: location map

Mine geology

The Mobrun Zn-Cu-Au-Ag Mine is located 30 km northeast of Rouyn-Noranda (Fig. 1). It was operated by Ressources Audrey Inc. until 1992, at which time Cambior Inc. became the operator. The deposit is hosted by a north-facing homoclinal sequence of felsic to mafic lava flows and felsic to intermediate pyroclastic rocks (Fig. 1; Caumartin and Caillé 1990; Riopel et al. 1990; Barrett et al. 1992; Larocque and Hodgson 1993). The rock units hosting the orebodies strike at 110° to 120° and dip subvertically (Fig. 2).

The deposit consists of three massive sulfide complexes: the 1100 orebody, the Main Lens, and the Satellite Lens Complex (Fig. 1). The respective grades and tonnages are listed in Table 1. The 1100 orebody is stratigraphically lowest and consists of 4 separate massive sulfide lenses, designated A, B, C, and D. The B lens, which contains the bulk of the mineralization, has a lateral extent near 300 m and a maximum thickness of 50 m in its central part. It extends downward from 360 m below surface and is open at depth (Fig. 2). The smaller A and D lenses are located stratigraphically above the B lens; the intermediate C lens is located stratigraphically below the B lens and also is open at depth. The outcropping Main Lens has a lateral extent of 350 m, a present vertical extent of 200 m, and a maximum width of 40 m in the core. The Satellite Lens Complex (SLC) comprises three massive sulfide bodies (Fig. 1) representing three parts of one originally continuous lens which was offset by northeast-striking faults. Synvolcanic hydrothermal alteration associated with the mineralization consists of chloritization, sericitization, silicification, and carbonatization (Caumartin and Caillé 1990; Riopel et al. 1990; Larocque and Hodgson 1993).

The structure of the rocks hosting the Mobrun deposit has been described by Caumartin and Caillé (1990) and Riopel et al. (1990). A regional schistosity (S1) oriented parallel to the strata is cut by a second schistosity (S2) which strikes east-west and dips steeply to the south. These fabrics are developed mainly in localized zones of intense deformation which follow the zones of altered rocks enveloping the Main and 1100 orebodies, and probably formed during the regional D2 deformation. Two major reverse fault zones striking 90° to 100° are present within the schist zone enveloping the Main Lens, one in the immediate hangingwall and one in the immediate footwall. A late fault system striking 020° to 040° cuts the strata, resulting in offsets of the Satellite Lens Complex (Fig. 1). Liaghat et al. (1993) proposed a temperature of deformation for the Main Lens of 300 °C and a pressure of 2 kb. These estimates are consistent with the results of a regional metamorphic study (W. Powell, personal communication 1993).

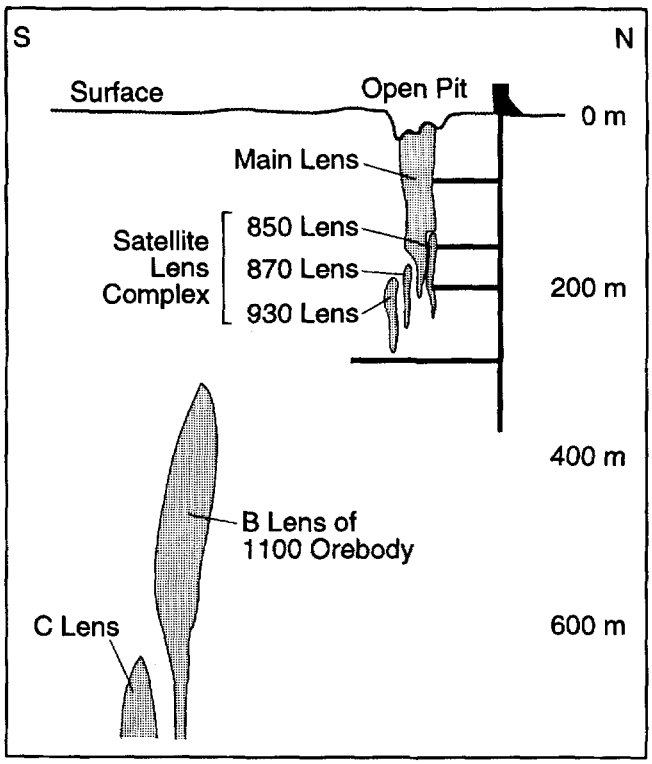

Fig. 2. Composite section showing the relative depths of the Mobrun orebodies (modified from Caumartin and Caillé 1990)

Table 1. Ore reserves, Mobrun Mine[a]

Orebody	Tonnes	Cu%	Zn%	Ag g/t	Au g/t
Satellite[b]	179,000	1.20	2.41	42.27	4.98
Main[b]	955,000	0.81	2.44	30.30	2.27
1100[c]	7,572,000	0.84	5.87	42.50	1.75
Total	8,706,000	0.84	5.42	41.12	1.87

[a] Provided by Ressources Audrey Inc.
[b] Proven reserves, February 1, 1989
[c] Probable reserves, October 25, 1991

Petrography of primary mineralization

In the Mobrun deposit, fourteen facies of mineralization have been identified (Table 2) which represent mappable subunits of the massive sulfide bodies (Larocque 1993; Larocque et al. 1993). The term "facies" refers to a distinct type of mineralization with specific mineralogical, textural, and structural characteristics (Fig. 3). These facies have genetic significance as they resulted from specific depositional or deformational processes (c.f., "sulfide lithofacies" of Brown and McClay 1993). Primary facies of mineralization resulted from synvolcanic hydrothermal and diagenetic processes and are similar to sulfide mineralization observed in modern seafloor and unmetamorphosed Kuroko deposits (Eldridge et al. 1983; Paradis et al. 1988; Peter and Scott 1988).

In the Mobrun orebodies, there is excellent preservation of primary facies of mineralization, given the state of deformation of the host rocks. These primary facies are overprinted locally by secondary facies resulting from metamorphism and deformation (Figs. 4, 5). Table 2 summarizes the characteristics of facies of mineralization in the Mobrun deposit. Some examples of primary facies are illustrated and described below in order to provide a basis for comparison with the facies resulting from metamorphism and deformation.

The main sulfide minerals in the Mobrun orebodies are pyrite, sphalerite, and chalcopyrite. Minor amounts of galena, arsenopyrite, digenite, and tetrahedrite have been observed. Magnetite occurs locally with chalcopyrite. Pyrrhotite is abundant towards the footwall of the B and C lenses of the 1100 orebody, but has not been observed in the Main and Satellite Lenses. Quartz, carbonate, chlorite, muscovite, and albite are the main non-sulfide minerals.

Bedded pyritic mineralization consists of micrometre-scale euhedra of pyrite in a matrix of chlorite (Fig. 3A), and resembles a well sorted sediment. Granular mineralization consists of micrometre- to millimetre-scale spheroids and spheroidal aggregates of pyrite in a matrix of

Table 2. Facies of mineralization in the Mobrun deposit[a]

Primary facies	Formed by deposition and reworking of sulphides by syn-volcanic hydrothermal fluids (syn-genetic/diagenetic)
Bedded pyrite	– μm-scale pyrite euhedra in chlorite matrix – apparent layering, "graded bedding"
Granular pyrite	– μm to mm-scale pyrite spheroids and spheroidal aggregates in matrix of sphalerite or gangue, internal colloform banding defined by porous pyrite, chalcopyrite, sphalerite, galena
Nodular pyrite	– mm- to cm-scale spherical bodies of pyrite in a sphalerite matrix – radiating internal structures
Massive fine pyrite	– microcrystalline to cryptocrystalline pyrite – colloform textures defined by porous pyrite, minor chalcopyrite, galena, sphalerite
Massive pyrite-chalcopyrite	– massive pyrite with unoriented replacement veins of chalcopyrite or pseudomorphic replacement of colloform/spheroidal pyrite by chalcopyrite
Massive sphalerite	– massive fine-grained sphalerite
Banded pyrite-sphalerite	– bands of massive sphalerite up to 10 cm wide, alternating with bands of granular, massive, or nodular pyrite
Banded pyrrhotite-pyrite	– bands of massive fine-grained pyrrhotite interlayered with granular pyrite
Banded pyrrhotite-sphalerite	– bands of massive pyrrhotite interlayered with massive sphalerite
Stringer mineralization	– veins, disseminations, and patches of chalcopyrite and/or pyrrhotite in altered wallrock
Secondary facies	**Formed during metamorphism and deformation**
Granular metablastic mineralization	– coarse-grained pyrite metacrysts in a matrix of gangue or other sulfides, metacrysts generally free of inclusions
Massive metablastic pyrite	– massive coarse pyrite with granuloblastic texture (triple junctions), some sutured grain boundaries
Foliated mineralization	– transgressive wispy bands of fine, abraded pyrite and discontinuous bands of angular pyrite
Transgressive veins and breccia zones	– subparallel and orthogonal sets of veins and veinlets, anastomosing networks of veinlets, vein breccias – contain any of pyrite, chalcopyrite, sphalerite, galena, electrum, quartz, chlorite, carbonate

[a] From Larocque [1993], modified from Larocque et al. [1993]

sphalerite or gangue (Fig. 3B). The spheroids exhibit complex internal structures consisting of cores and concentric bands of sulfides (chalcopyrite, sphalerite, and galena) and gangue, similar to features described by Lianxing and McClay (1992). Massive fine pyrite consists of microcrystalline to crypocrystalline pyrite which locally contains chalcopyrite, sphalerite, and galena in colloform bands (Fig. 3C). Banded pyrite – sphalerite comprises bands of massive fine-grained sphalerite alternating with bands of granular or massive pyrite (Fig. 3D). Pyrrhotite-bearing primary facies consist of massive pyrrhotite interlayered with either granular pyrite or massive sphalerite.

Results of metamorphism and deformation

The characteristics of secondary facies of mineralization are a function of the degree and style of deformation to which primary facies were subjected. In general, mechanisms of deformation may be divided into mechanical and chemical processes. Mechanical processes that accomodate strain include brittle deformation (brittle failure, cataclastic flow, grain-boundary sliding) and ductile deformation (dislocation glide, dislocation creep, deformation twinning); chemical processes include diffusive mass transfer (lattice-diffusion creep, grain-boundary diffusion creep, solution-precipitation creep) (Vokes 1969; McClay 1977; Poirier 1985; Cox 1987; Gilligan and Marshall 1987). Both mechanical and chemical deformation mechanisms, as well as recovery processes (e.g., subgrain formation, postdeformational recrystallization), were responsible for the modification of primary facies of mineralization in the Mobrun deposit.

Mechanical processes

The most commonly observed facies of mineralization in the Mobrun deposit that resulted from brittle deformation consists of transgressive veins and breccia zones. These formed as fillings in tectonically generated dilatancies caused by high fluid-pressure. These fracture-fillings of varying widths developed mainly in massive pyrite, and commonly occur in orthogonal or subparallel sets (Fig. 4). On the basis of form, the veins can be subdivided into simple planar veinlets (< 1 cm thick) and veins (> 1 cm thick), anastamosing networks of veinlets filling fractures or replacing recrystallized grain boundaries (see below), and vein breccias in which fragments of pyrite float in a matrix of non-sulfide and sulfide minerals. The veins and matrix material in the breccia zones consist of remobilized ore constituents and gangue minerals, including any of pyrite, chalcopyrite, sphalerite, galena, electrum, quartz, carbonate, and chlorite (Figs. 4, 5A).

Cataclastic flow resulted in the development of foliated pyritic mineralization in the Mobrun deposit (Figs. 5B,C). This facies consists of transgressive, wispy, commonly kinked bands of fine-grained pyrite in a chloritic matrix. These bands alternate with discontinuous bands of coarser-grained angular pyrite in a matrix of quartz and

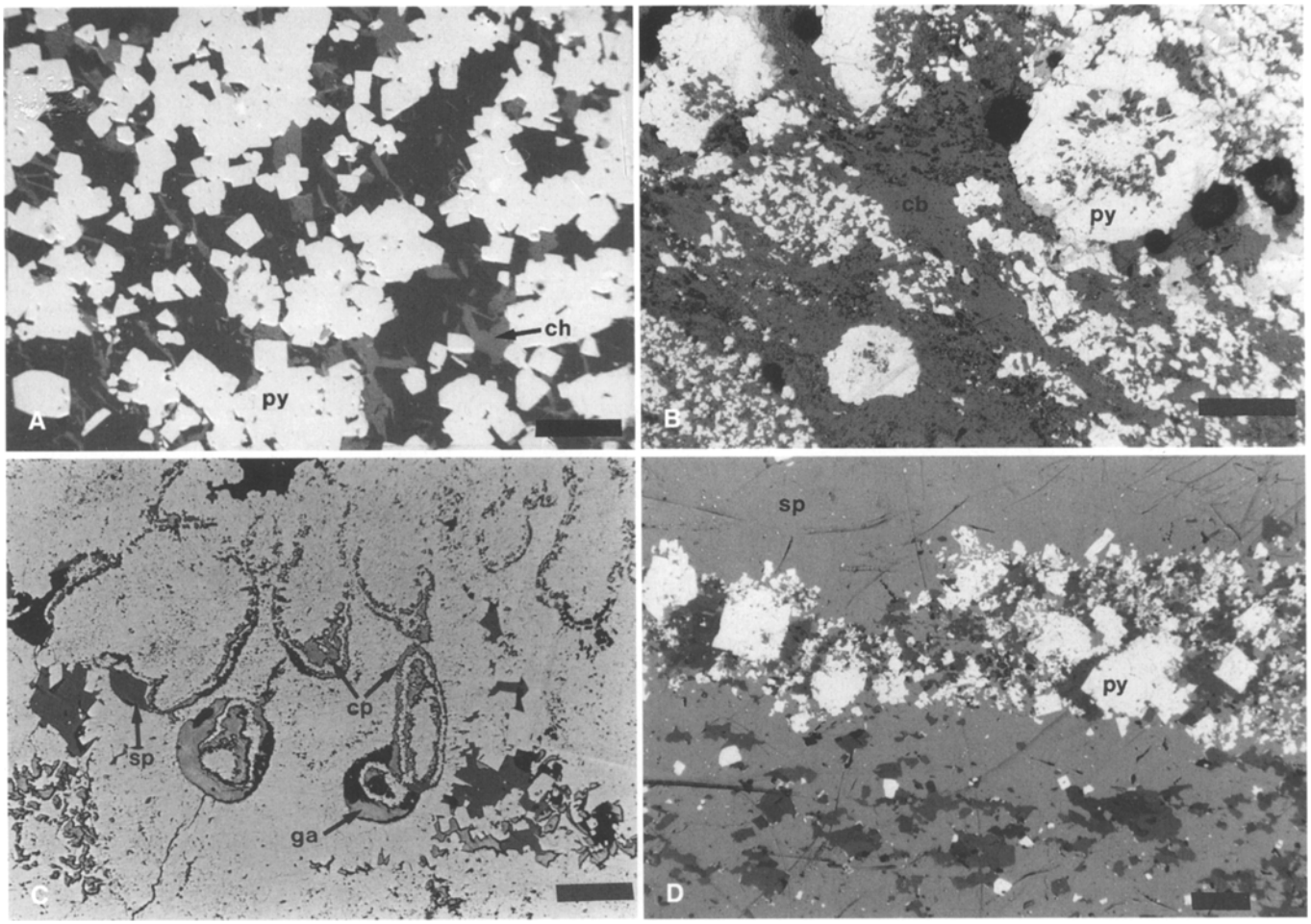

Fig. 3A–D. Reflected-light photomicrographs and scanning electron microscope (SEM) backscatter electron (BSE) images of primary facies of mineralization. Lengths of scale bars (*lower right*) in parentheses (*py* pyrite, sp sphalerite, cp chalcopyrite, *ga* galena, *ch* chlorite, *cb* carbonate). **A** Bedded pyritic mineralization consisting of pyrite euhedra in a matrix of chlorite (50 μm). **B** Granular pyritic mineralization consisting of spheroidal bodies of pyrite in a matrix of carbonate. Primary layering from upper left to lower right (500 μm). **C** Massive fine pyrite with colloform banding defined by galena, chalcopyrite and sphalerite (100 μm). **D** Banded pyrite – sphalerite consisting of massive fine-grained sphalerite and granular to euhedral pyrite (200 μm)

chlorite. Individual pyrite grains in chloritic bands are rounded (Fig. 5C) due to abrasion that occurred during shearing (Vokes 1969; Cox 1987). This facies likely resulted from deformation of primary facies containing brittle sulfides in a ductile matrix, such as bedded or granular pyrite; deformation of the ductile chloritic matrix would have facilitated the rounding of brittle grains of pyrite within the matrix.

Evidence of ductilely deformed sulfides co-existing with sulfides which underwent brittle deformation has been observed on a number of scales in the Mobrun deposit. For example, in a stope-face in the Satellite Lens Complex, parallel sets of quartz-chalcopyrite veins crosscut zones of massive pyrite, but are absent in intervening sphalerite-rich zones (see Larocque et al. 1993, Fig. 6). This juxtaposition of deformational style has also been observed in thin section, where brittle fractures in a band of pyrite bounded by unfractured massive sphalerite are filled by chalcopyrite (Fig. 5D). In addition, the sphalerite matrix containing granular pyrite in Fig. 6A deformed ductilely (likely by dislocation gliding), resulting in pressure-solution of the brittle grains of pyrite (see below). These observations are consistent with the estimates of temperature and pressure of deformation by Liaghat et al. (1993). Under lower greenschist-facies conditions, pyrite exhibits brittle behaviour, whereas sphalerite deforms ductilely (Marshall and Gilligan 1987, Fig. 4).

Chemical processes

Recrystallization of pyrite resulted in the development of granular and massive metablastic mineralization. Granular metablastic mineralization consists of coarse-grained, commonly idioblastic, pyrite metacrysts (Craig and Vokes 1992; Vokes and Craig 1993) which generally are free of inclusions. The pyrite metacrysts are surrounded by a matrix comprising other sulfide or gangue minerals (Figs. 6A,B), and likely formed by static recrystallization of primary granular pyrite. They commonly exhibit subparallel intragranular extension microfractures (Cox 1987) which are filled with chalcopyrite (Fig. 6B). Caries-

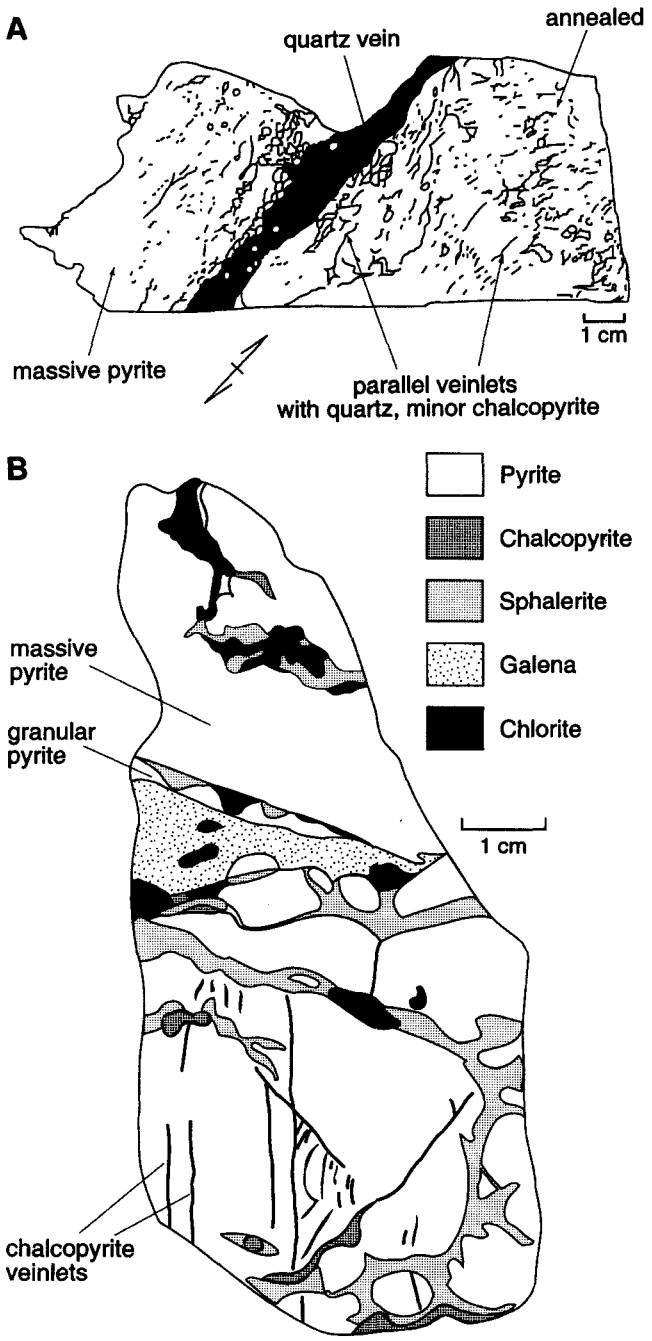

Fig. 4A, B. Sketches of hand specimens containing secondary veins. **A** Parallel vein and veinlets of quartz cutting massive fine pyrite. **B** Multiple generations of veins cutting massive fine pyrite. Early chalcopyrite veinlets are crosscut by later polymetallic veins (containing galena, sphalerite, chalcopyrite, and chlorite)

like growth embayments indicative of metablastic growth (Vokes and Craig 1993) also have been observed (Fig. 6A). The presence of ductile matrix sulfides or gangue resulted in fracturing (due to grain-boundary sliding) and indentation (due to pressure-solution) along grain boundaries in brittle pyrite metacrysts (Fig. 6A). Bulging grain boundaries (Fig. 6A) suggest that dynamic recrystallization of granular pyrite also occurred (Cox et al. 1981; Cox 1987).

A variation of granular metablastic mineralization consists of overgrowths of pyrite on cores of primary granular pyrite (Figs. 6C,D). The overgrowths commonly exhibit textures different than those in the cores of grains. For example, spongey pyrite has been observed as overgrowths on featureless grains of pyrite (Fig. 6C), and massive, inclusion-free pyrite has been observed rimming pyrite with a random or concentric arrangement of inclusions (Fig. 6D). While it is possible for overgrowths to have formed during diagenesis (e.g., hydrothermal reworking in the syngenetic sulfide pile), the preferred orientation of many of the overgrowths indicate that they formed as a result of solution-precipitation creep during synkinematic metamorphism. In addition, euhedral metablastic pyrite overgrowths on foliated mineralization in the 1100 Lens (Fig. 6E) suggest that cataclastic flow predated metablastesis. Some pyrite metacrysts associated with foliated mineralization are surrounded by pyrite-free boundary layers which are thickest parallel to the local foliation direction (Fig. 6F), indicating anisotropy of diffusion rates parallel and perpendicular to a pre-existing foliation (Cook et al. 1993).

Massive metablastic mineralization consists of massive, generally inclusion-free, pyrite or pyrrhotite exhibiting granuloblastic or "foam" texture (Stanton 1964) with triple junctions indicative of recrystallization (Fig. 6G). These recrystallization textures likely formed by thermal annealing of deformed grain aggregates (c.f. Lianxing and McClay 1992). It is possible for recrystallization to occur during synvolcanic hydrothermal reworking. However, presence of elongate grain-fabric (Fig. 6G) and sutured grain boundaries (Fig. 6H) resulting from solution-precipitation creep indicate that recrystallization occurred under directed pressure during metamorphism (Vokes 1969; Cox 1987; Vokes and Craig 1993). The presence of subgrain structure in some samples containing recrystallized pyrite indicates that the recrystallization was dynamic rather than static (Cox 1987). In other samples, annealed or sutured grain boundaries appear to have opened up, either due to tectonic deformation or fluid pressure (Vokes and Craig 1993). The dilatant zones subsequently were filled and grain boundaries replaced by chalcopyrite (Fig. 6H).

In addition to textural changes resulting from recrystallization and pressure-solution, chemical changes occurred during metamorphism and deformation of the Mobrun deposit. Ion-microprobe analysis of sulfides has established that syngenetic gold is present in the orebodies, and that metamorphic recrystallization of pyrite resulted in the release of invisible gold and its subsequent deposition in tectonic veins in electrum and secondary chalcopyrite (Larocque et al., 1995). Petrographic and chemical evidence indicate that the extent of metamorphic remobilization (i.e., distance of transport) was small in the Main and Satellite Lenses, but on the order of hundreds of metres in the 1100 Lens (Larocque et al. 1993).

Discussion

There is restricted development of secondary facies in the Main and Satellite Lenses, and those facies that are

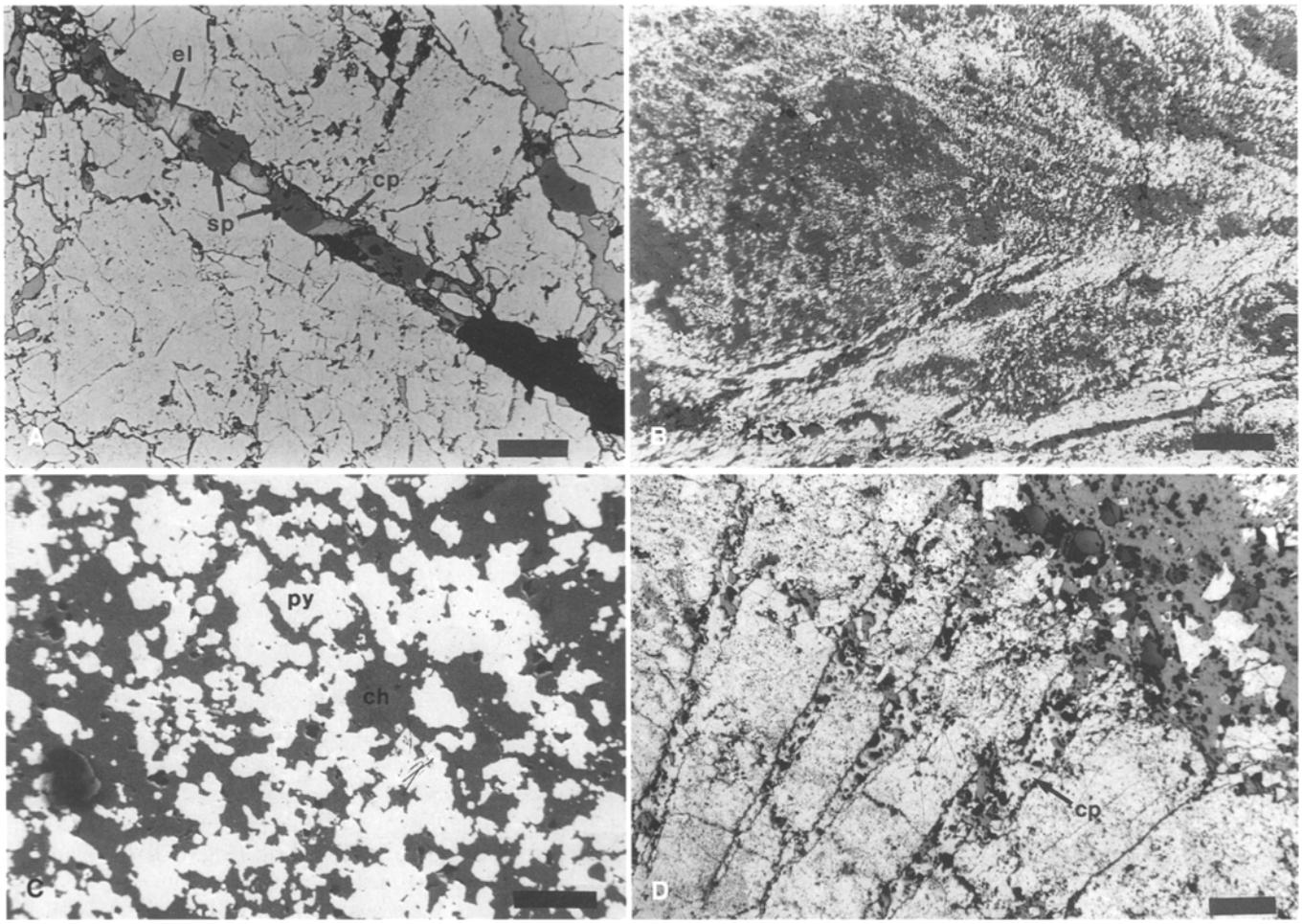

Fig. 5A–D. Reflected-light photomicrographs and SEM BSE images of secondary facies of mineralization resulting from mechanical processes. Lengths of *scale bars* in parentheses (*py* pyrite, *sp* sphalerite, *cp* chalcopyrite, *el* electrum). **A** Massive fine pyrite cut by veinlet containing chalcopyrite, sphalerite and electrum (200 μm). **B** Foliated pyritic mineralization comprising wispy bands consisting of rounded grains of pyrite (*white*) in a chloritic matrix (*dark grey*), developed during shearing (250 μm). **C** Rounded (abraded) grains of pyrite and chloritic matrix in foliated pyritic mineralization (50 μm). **D** Millimetre-thick band of pyrite in massive sphalerite contains veinlets of chalcopyrite filling parallel fractures. Surrounding sphalerite contains no veinlets, having deformed ductilely (1 mm)

observed resulted mainly from mechanical processes. Transgressive veins resulting from brittle failure of massive pyrite are the most abundant of the secondary facies in these lenses. Ductile deformation of sphalerite (likely accomplished by dislocation gliding) also occurred. Evidence of cataclastic flow and static recrystallization of pyrite are present but rare. In contrast, although the 1100 Lens exhibits significant preservation of primary facies, development of secondary facies resulting from *both* mechanical and chemical processes is pronounced. Transgressive veins and zones of dynamic and static recrystallization and metablastic growth are abundant. Zones of foliated mineralization resulting from cataclastic flow exhibit restricted development, present only in the flanks and stratigraphic hangingwall and footwall of the massive sulfide bodies. Evidence of solution-precipitation creep commonly was observed in the 1100 orebody, especially at the eastern end of the B lens (Larocque 1993).

The distribution of secondary facies at Mobrun is controlled at least in part by the rheological properties of the primary facies affected, and the rheological properties of surrounding rocks. Observations at Mobrun are consistent with the fact that sphalerite deforms ductilely under greenschist-facies metamorphic conditions (Clark and Kelly 1973), whereas pyrite undergoes brittle deformation (Atkinson 1975; Cox 1987). Where pyrite was in a matrix of sphalerite in the Mobrun orebodies, strain was accomodated by ductile flow of sphalerite, and pyrite was unaffected. In contrast, zones of massive pyrite deformed brittly under the same conditions. This is significant because brittle deformation of pyrite facilitated development of fractures which provided depositional sites for remobilized gold and sulfides.

Differences in primary ore assemblages and textures among the various orebodies account for some of the differences in the degree of development of secondary facies of mineralization. However, some differences appear to be the result of gradients in metamorphic conditions within the mine. Robert and Brown (1986) and Powell et al. (1993) have presented evidence for the subhorizontal orientation of regional metamorphic isograds in the Abitibi province. Given that most volcanic strata in the

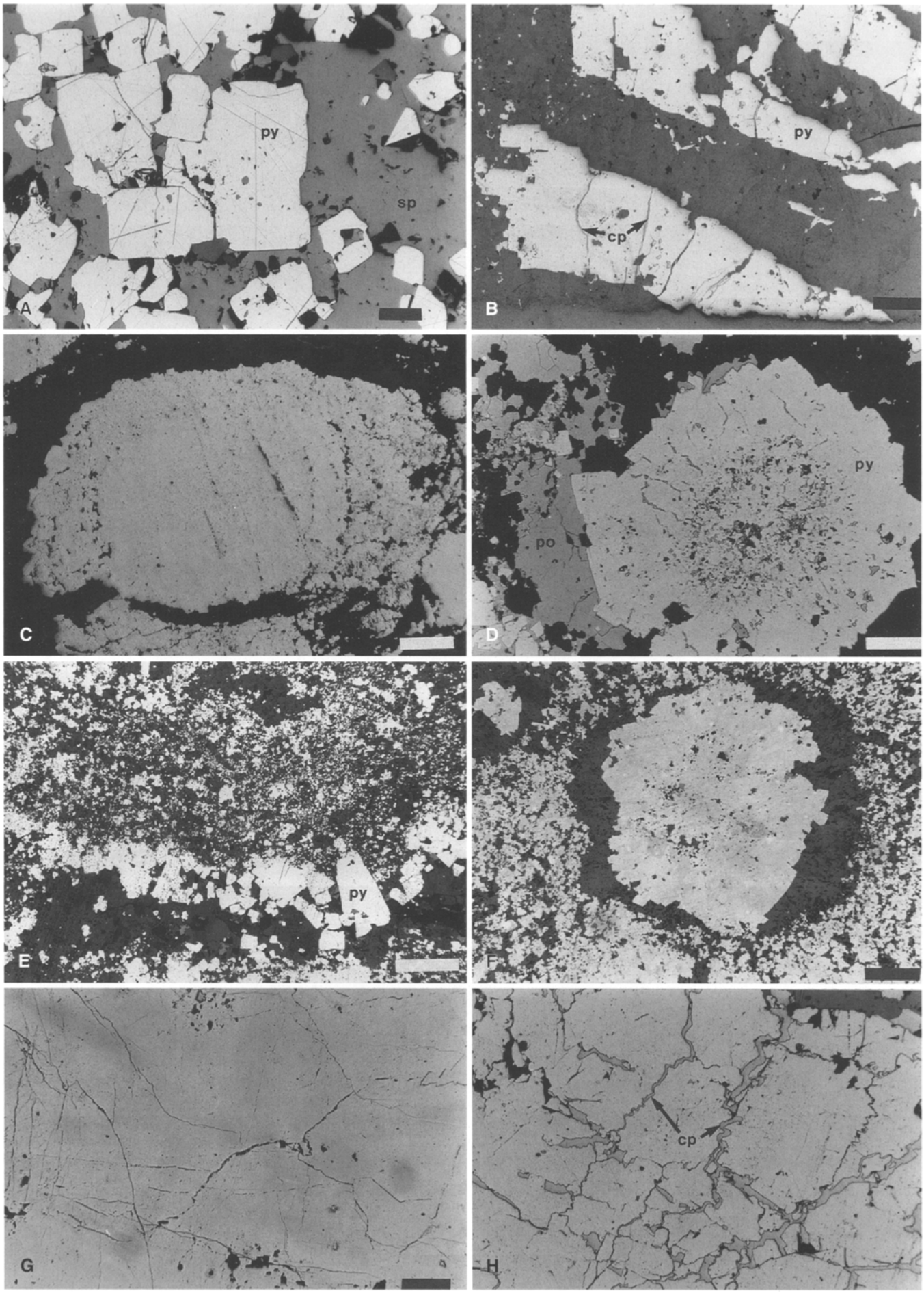
py
sp
A
py
cp
B
C
py
po
D
py
E
F
G
cp
H

Abitibi dip subvertically, their results indicate that the assemblages observed must have formed during late- to post-tectonic metamorphism rather than during initial burial of the volcanic pile. This may explain why the 1100 Lens of the Mobrun deposit appears to have been subjected to more intense metamorphism than the other lenses. Whereas the Main and Satellite Lenses outcrop or subcrop, the upper part of the 1100 Lens is at a depth of 300 m, below the lowermost extensions of the Main and Satellite Lenses (Fig. 2). Thus, the 1100 Lens was subjected to slightly higher temperatures and confining pressures during metamorphism than the other lenses.

This fact could account for the presence of pyrrhotite in the 1100 Lens, and the lack of it in the other lenses, as many early workers interpreted pyrrhotite as a metamorphic product of the breakdown of pyrite. However, the lack of breakdown textures of pyrite in the 1100 Lens and the documentation of pyrrhotite in modern seafloor deposits (Lonsdale et al. 1980) support the interpretation that pyrrhotite in the 1100 Lens is primary. Also, the distribution of pyrrhotite on the property-scale at Mobrun is similar to that in the Noranda camp as a whole: relatively gold-poor pyrite-pyrrhotite ores occur lower in the stratigraphy, whereas pyritic ores with higher gold grades occur higher in the stratigraphy.

Other factors which may influence deformational style include fluid activity and permeability within the zone of deformation (Ashby and Verrall 1973; Duckworth and Rickard 1993). In some metamorphic environments, the deformation process is controlled by mass transfer in an advecting fluid phase, and the deformation rate is determined by the rate of fluid flow (Etheridge et al. 1984). At Mobrun, the evidence for extensive metamorphic remobilization of ore constituents and significant fluid-ore interactions (Larocque et al. 1993, 1995), as well as the presence of ore textures resulting from solution-precipitation, indicate that fluids were abundant in the area of the 1100 Lens during metamorphism and deformation. In contrast, the Main Lens does not appear to have been affected much by fluids. The amount of interaction between fluids and each of the ore lenses may be related to the relative thicknesses and volumes of the orebodies compared to their host rocks. Both the Main and 1100 Lenses are hosted by pyroclastic rocks (which had a relatively high primary permeability) overlain and underlain by less permeable rhyolitic lava flows (Fig. 1). The pyroclastic units likely acted as horizons of enhanced or focussed fluid-flow. There is a greater thickness of pyroclastic rocks overlying the Main Lens through which fluids could have flowed, compared to the relatively small thickness of pyroclastic rocks underlying the 1100 Lens (Fig. 1). Thus, the 1100 Lens may have interacted more extensively with metamorphic fluids because there was less space for the fluids to flow around the orebody.

Fig. 6A–H. Reflected-light photomicrographs images of secondary facies resulting from chemical processes. *Scale bars* represent 500 μm unless specified otherwise (*py* pyrite, *sp* sphalerite, *cp* chalcopyrite, po pyrrhotite). **A** Penetration of large pyrite metablast by two smaller metablasts due to ductile deformation of sphalerite and pressure solution of pyrite. Small metablasts with caries-like growth embayments at top left and bottom right. Grain-boundary bulging indicative of dynamic recrystallization at top middle and bottom middle (250 μm). **B** Pyrite metablasts with subparallel veinlets of chalcopyrite. **C** Spongey pyrite overgrowth on massive metablastic core. Overgrowth is thickest parallel to foliation direction (foliation direction parallel to long axis of photo). **D** Pyrite metablast with relict concentric arrangement of inclusions in core and inclusion-free metamorphic overgrowth. **E** Foliated pyrite resulting from cataclastic flow with overgrowths of metablastic pyrite. **F** Pyrite metablast separated from foliated pyrite by a concentric zone depleted in pyrite. The depleted zone is thickest parallel to the foliation (i.e., parallel to long axis of photo) and thinnest at right angles to the foliation. **G** Triple junctions ("foam texture") developed in massive metablastic pyrite. Flattening perpendicular to long axis of photo. **H** Polygonized and recrystallized massive pyrite with sutured grain boundaries replaced by chalcopyrite veinlets (100 μm)

Conclusions

Greenschist-facies metamorphism of the Mobrun deposit resulted in changes in ore textures, development of tectonic structures, remobilization of gold and sulfides, and formation of a new mineral (electrum).

Textures and structures resulting from brittle deformation (e.g., brittle failure, cataclastic flow), ductile deformation (e.g., dislocation glide, dislocation creep), and recrystallization (static and dynamic) are present in the Mobrun orebodies.

Both mechanical and chemical processes operated during deformation and metamorphism of the deposit. The Main and Satellite Lenses were affected mainly by mechanical processes, whereas the 1100 Lens was affected by both mechanical and chemical processes.

The higher degree of development of secondary facies of mineralization (especially those resulting from chemical processes) in the 1100 Lens relative to the other lenses may be due to its greater depth (as regional metamorphic isograds are subhorizontal) and more extensive interactions with metamorphic fluids (possibly resulting from enhanced flow through the 1100 Lens).

Acknowledgements. We appreciate the assistance of geological and mine personnel at Ressources Audrey Inc., Mine Mobrun, and Minnova Inc, especially Michel Bouchard and Gérald Riverin. At Los Alamos National Lab, Jim Stimac kindly provided access to a photographic microscope and Ruth Bigio carried out computer-aided drafting of figures. The manuscript benefitted from discussions with Karen Carter at Los Alamos National Lab, and from comments by two anonymous reviewers. Financial support was provided by Ressources Audrey Inc., Minnova Inc., and the Natural Science and Engineering Research Council of Canada, through a Collaborative Research and Development Grant awarded to C.J. Hodgson.

References

Ashby, M.F., Verrall, R.A. (1973) Diffusion accomodated flow and superplasticity. Acta Metall. 21:149–163.

Atkinson, B.K. (1975) Experimental deformation of polycrystalline pyrite: effects of temperature, confining pressure, strain rate, and porosity. Econ. Geol. 70:473–487.

Barrett, T.J., Cattalani, S., Hoy, L., Riopel, J., Lafleur, P.-J. (1992) Massive sulfide deposits of the Noranda area, Quebec: IV. The Mobrun Mine. Can. J. Earth Sci. 29:1349–1374.

Brown, D., McClay, K.R. (1993) Deformation textures in pyrite from the Vangorda Pb-Zn-Ag deposit, Yukon, Canada. Mineral. Mag. 57:55–66.

Caumartin, C., Caillé, M.-F. (1990) Volcanic stratigraphy and structure of the Mobrun Mine. In: Rive, M., Verpaelst, P., Gagnon, Y., Lulin, J.-M., Riverin, G., Simard A., (eds.) The northwestern Quebec polymetallic belt: a summary of 60 years of mining exploration. Can. Inst. Min. Metall., Spec. Vol. 43:119–132

Clark, B.R., Kelly, W.C. (1973) Sulfide deformation studies. I. Experimental deformation of pyrrhotite and sphalerite to 2,000 bars and 500 °C. Econ. Geol. 84:1684–1689

Cook, N.J., Halls, C., Boyle, A.P. (1993) Deformation and metamorphism of massive sulfides at Sulitjelma, Norway. Mineral. Magazine 57:67–81

Cox, S.F. (1987) Flow mechanisms in sulfide minerals. Ore Geol. Rev. 2:133–171

Cox, S.F., Etheridge, M.A., Wall. V.J. (1981) The experimental ductile deformation of polycrystalline and single crystal pyrite. Econ. Geol. 76:2105–2117

Craig, J.R., Vokes, F.M. (1992) Ore mineralogy of the Appalachian – Caledonian stratabound sulfide deposits. Ore Geol. Rev. 7: 77–123

Craig, J.R., Vokes, F.M. (1993) The metamorphism of pyrite and pyritic ores: an overview. Mineral. Magazine 57:3–18

Dimroth, E., Imreh, L., Rocheleau, M., Goulet, N. (1983a) Evolution of the south-central segment of the Archean Abitibi Belt, Québec. II. Tectonic evolution and geomechanical model. Can. J. Earth Sci. 20:1355–1373

Dimroth, E., Imreh, L., Rocheleau, M., Goulet, N. (1983b) Evolution of the south-central segment of the Archean Abitibi Belt, Québec. III. Plutonic and metamorphic evolution and geotectonic model. Can. J. Earth Sci. 20:1374–1388

Duckworth, R.C., Rickard, D. (1993) Sulfide mylonites from the Renström VMS deposit, Northern Sweden. Mineral. Mag. 57:83–91

Eldridge, C.S., Barton, P.B., Jr., Ohmoto, H. (1983) Mineral textures and their bearing on formation of the Kuroko orebodies. Econ. Geol. Monogr 5:241–281

Etheridge, M.A., Wall, V.J., Cox, S.F., Vernon, R.H. (1984) High fluid pressures during regional metamorphism and deformation – implications for mass transport and deformation mechanisms. J. Geophys. Res. 89:4344–4358

Gélinas, L., Trudel, P., Hubert, C. (1984) Chimico-stratigraphie et tectonique du Groupe de Blake River. Min. L'Energie Ress. Québec., MM 83–91, 41 pp

Gilligan, L.B., Marshall, B. (1987) Textural evidence for remobilization in metamorphic environments. Ore Geol. Rev. 2:205–229

Hubert, C., Trudel, P., Gélinas, L. (1984) Archean wrench-fault tectonics and structural evolution of the Blake River Group, Abitibi Belt. Can. J. Earth Sci. 21:1024–1032

Jolly, W.T. (1978) Metamorphic history of the Archean Abitibi belt. Geol. Surv. Canada Paper 78–10:63–78

Jolly, W.T. (1980) Development and degradation of Archean lavas, Abitibi area, Canada, in light of major element geochemistry. J. Petrol. 21:323–363

Kelly, W.C., Clark, B.R. (1975) Sulfide deformation studies. III. Experimental deformation of chalcopyrite to 2,000 bars and 500 °C. Econ. Geol. 70:431–453

Knipe, R.J. (1989) Deformation mechanisms – recognition from natural tectonites. J. Struct. Geol. 11:127–146

Larocque, A.C.L. (1993) The geological controls of gold distribution in the Mobrun volcanic-associated massive sulfide deposit, Rouyn-Noranda, Quebec. Unpublished Ph.D. thesis, Queen's University, Kingston, Ontario, 232 pp

Larocque, A.C.L., Hodgson, C.J. (1993) Carbonate-rich footwall alteration at the Mobrun mine, a possible Mattabi-type VMS deposit in the Noranda camp. Can. Inst. Mining Metall. Explor. Min. Geol. J. 2:165–169

Larocque, A.C.L., Hodgson, C.J., Lafleur, P.-J. (1993) Gold distribution in the Mobrun VMS deposit, Noranda, Quebec: a preliminary evaluation of the role of metamorphic remobilization. Econ. Geol. 88:1443–1459

Larocque, A.C.L., Hodgson, C.J., Cabri, L.J., Jackman, J.A. (1995) Ion-microprobe analysis of pyrite, chalcopyrite and pyrrhotite from the Mobrun VMS deposit in northwestern Quebec: evidence for metamorphic remobilization of gold. Can. Mineral. 33:373–388

Liaghat, S., Brown, A.C., Hubert, C. (1993) Deformation imprints upon sulfide mineral assemblages at the Mobrun massive sulfide deposit, Noranda District, Quebec. Geol. Assoc. Canada/Mineral. Assoc. Canada, Progr. Abstr. 18:A59

Lianxing, G., McClay, K.R. (1992) Pyrite deformation in stratiform lead-zinc deposits of the Canadian Cordillera. Mineral. Deposita 27:169–181

Lonsdale, P.F., Bischoff, J.L., Burns, V.M., Kastner, M., Sweeney, R.E. (1980) A high-temperature hydrothermal deposit on the seabed at a Gulf of California spreading centre. Earth Planet. Sci. Lett. 49:8–20

Marshall, B., Gilligan, L.B. (1987) An introduction to remobilization: Information from ore-body geometry and experimental considerations. Ore Geol. Rev. 2:87–131

McClay, K.R. (1977) Pressure solution and Coble creep in rocks and minerals: a review. J. Geol. Soc. Lond. 134:57–70.

McClay, K.R. (1991) Deformation of stratiform Zn-Pb (-barite) deposits in the northern Canadian Cordillera. Ore Geol. Rev. 6:435–462

Ministère de l'Energie et des Ressources du Québec – Ontario Geological Survey (1984) Carte lithostratigraphique de la Sous-province de l'Abitibi: DV 83–16, 1:500,000

Mookherjee, A. (1976) Ores and metamorphism: temporal and genetic relationships. In: Wolf, K.H. (ed.) Handbook of stratiform and stratabound ore deposits, vol. 4. Tectonics and metamorphism. Elsevier, Amsterdam, New York, pp. 203–260

Paradis, S., Jonasson, I.R., Le Cheminant, G.M., Watkinson, D.H. (1988) Two zinc-rich chimneys from the Plume Site, southern Juan de Fuca Ridge. Can. Mineral. 26:637–654

Peter, J.M., Scott, S.D. (1988) Mineralogy, composition, and fluid-inclusion microthermometry of seafloor hydrothermal deposits in the Southern Trough of Guaymas Basin, Gulf of California. Can. Mineral. 26:567–587

Poirier, J.-P. (1985) Creep of crystals. Cambridge University Press, Cambridge, 260 pp

Powell, W.G., Hodgson, C.J., Carmichael, D.M. (1993) Low-temperature metamorphism and its relationship to the Larder Lake – Cadillac Break, Matachewan area, Abitibi belt, Ontario, Canada. J. Metamorphic Geol. 11:165–178

Riopel, J., Hubert, C., Cattalani, S., Barrett, T.J., MacLean, W.H. (1990) Métallogénie des gisements de métaux usuels dans la ceinture de roches vertes de l'Abitibi, nordouest Québecois. IV. La mine Mobrun lentille principale, Noranda, Québec. Inst. Recherche Explo. Minérale Projet no. 82–43G, 1988–89. Min. Energie Ress. Québec, Juillet 1990

Riverin, G., and Hodgson, C.J. (1980) Wallrock alteration at the Millenbach Cu-Zn mine, Noranda, Québec. Econ. Geol. 75:424–444

Robert, F., Brown, A.C. (1986) Archean gold-bearing quartz veins at the Sigma mine, Abitibi greenstone belt, Quebec. I. Geologic relations and formation of the vein system. Econ. Geol. 81:578–592

Roscoe, W.E. (1975) Experimental deformation of natural chalcopyrite at temperatures up to 300 °C over the strain rate range 10^{-2} to 10^{-6} sec^{-1}. Econ. Geol. 70:454–472.

Rosen-Spence, A.F. de (1976) Stratigraphy, development and petrogenesis of the central Noranda volcanic pile, Noranda, Québec. Unpublished Ph.D. thesis, Univ. of Toronto, Toronto, Ontario, 166 pp

Stanton, R.L. (1964) Mineral interfaces in stratiform ores. Trans. Inst. Mining Metall. 74:45–79

Vokes, F.M. (1969) A review of the metamorphism of sulfide deposits. Earth Sci. Rev. 5:99–143

Vokes, F.M., Craig, J.R. (1993) Post-recrystallization mobilization phenomena in metamorphosed stratabound sulfide ores. Mineral. Mag. 57:19–28

Editorial handling: R. Kerrich